(7) Gros, L.; Ringsdorf, H.; Schupp, H. *Angew. Chem., Int. Ed. Engl.* **1981**, *20*, 305–325.
(8) Fendler, J. H. *Science (Washington, D.C.)* **1984**, *223*, 888–894.
(9) Fuhrhop, J. H.; Mathieu, J. *Angew. Chem., Int. Ed. Engl.* **1983**, *23*, 100–113.
(10) Fendler, J. H. "Membrane Mimetic Chemistry"; Wiley-Interscience: New York, 1982.
(11) Fendler, J. H. *Chem. Eng. News* **1984** (Jan 2), *62*, 25–38.
(12) Fendler, J. H. *Acc. Chem. Res.* **1980**, *13*, 7–13.
(13) Reed, W.; Guterman, L.; Tundo, P.; Fendler, J. H. *J. Am. Chem. Soc.* **1984**, *106*, 1897–1907.
(14) Nome, F.; Reed, W.; Politi, M.; Tundo, P.; Fendler, J. H. *J. Am. Chem. Soc.* **1984**, *106*, 8086–8093.
(15) Nome, F.; Reed, W.; Fendler, J. H. *J. Am. Chem. Soc.*, submitted.
(16) Reed, W.; Lasic, D.; Hauser, H.; Fendler, J. H. *J. Am. Chem. Soc.*, submitted.
(17) Yau, W. W.; Kirkland, J. J.; Bly, D. D. "Modern Size-Exclusion Liquid Chromatography"; Wiley: New York, 1979.
(18) Effects of morphological changes on vesicle photopolymerization are the subject of our current investigations.
(19) Gaub, H.; Sackmann, E.; Buschl, R.; Ringsdorf, H. *Biophys. J.* **1984**, *45*, 725–731.
(20) de Gennes, P.-G. "The Physics of Liquid Crystals", 2nd ed.; Oxford University Press: Oxford, 1974.
(21) Galla, H.; Sackmann, E. *J. Am. Chem. Soc.* **1975**, *97*, 4114–4118.
(22) Gebhardt, C.; Gruler, H.; Sackmann, E. *Z. Naturforsch. C: Biosci.* **1977**, *32C*, 581–596.
(23) Reed W. Dissertation, Clarkson University, 1984.
(24) Bolikal, D.; Regen, S. *Macromolecules* **1984**, *17*, 1287–1289.
(25) Dorn, K.; Patton, E. V.; Klingbiel, R. T.; O'Brien, D. F.; Ringsdorf, H. *Makromol. Chem., Rapid Commun.* **1983**, *4*, 513–517.

Effects of Photopolymerization on Surfactant Vesicle Surface Morphology

Wayne Reed,[1] Danilo Lasic,[2] Helmut Hauser,[2] and Janos H. Fendler*[1]

Department of Chemistry and Institute of Colloid and Surface Science, Clarkson University, Potsdam, New York 13676, and Laboratorium fur Biochemie, Eidgenossische Technische Hochschule, CH-8092 Zurich, Switzerland. *Received December 19, 1984*

ABSTRACT: Properties of vesicles and polymerized vesicles prepared from $[C_{15}H_{31}CO_2(CH_2)_2]N^+(CH_3)CH_2C_6H_4CH{=}CH_2,Cl^-$ (1) have been investigated by transient dichroism and electron paramagnetic resonance measurements using erythrosin, 5-doxylstearic acid [FA(12,3)], and 5-doxylphosphatidylcholine [PC(12,3)] as reporters. Erythrosin added to nonpolymerized 1 vesicles showed no rotation anisotropy over the millisecond time domain. Conversely, erythrosin added to polymerized 1 vesicles showed marked temperature-dependent anisotropies. At room temperature, the time dependence of polarization anisotropy, $r(t)$, rose to a plateau value over the 0.5-ms time scale. At higher temperatures the plateau was lost and the anisotropy decay became measurable. Plots of anisotropy decays vs. temperature indicated the occurrence of a phase transition at 33 °C. The rise of $r(t)$ was rationalized by assuming the partitioning of erythrosin among different environments with different lifetimes and anisotropies. The temperature dependence of the hyperfine splitting of FA(12,3) and PC(12,3) added to sonicated 1 vesicles indicated phase transitions at 26.5 and 31.0 °C. Examination of FA(12,3) added to polymerized 1 vesicles indicated a phase transition temperature of 35 °C. Hyperfine splittings of PC(12,3) added to polymerized 1 vesicles decreased almost linearly with increasing temperatures, indicating a considerable broadening of the phase transition reported. At 25 °C, both spin probes appear to be less immobilized in polymerized than in nonpolymerized vesicles. This observation coupled with the transient dichroism of erythrosin substantiated the proposed formation of clefts on the vesicle surfaces upon photopolymerization. Differential scanning calorimetry of multicompartment 1 vesicles (prepared by vortexing 1) indicated a phase transition temperature at 35 °C. Upon polymerization the transition broadened and the gel-to-liquid phase transition temperature increased to 65 °C. These data indicate intrabilayer polymerizations in multicompartment vesicles.

Introduction

Full realization of the potentials of polymerized surfactant vesicles[3–7] demands a detailed understanding of their structures and of the mechanisms of their formation. Recently, we reported the kinetic consequences of the photolysis of vesicles prepared from a surfactant that contained a styrene moiety in its head group: $[C_{15}H_{31}CO_2(CH_2)_2]_2N^+(CH_3)CH_2C_6H_4CH{=}CH_2,Cl^-$ (1).[8] The observed first-order disappearance of the styrene absorbances have been found to be independent of the vesicle concentration and have been discussed, therefore, in terms of two-dimensional intravesicular surface polymerizations.[8] Flash photolysis of argon-bubbled vesicular solutions of 1 by 15-ns, 266-nm, 2-mJ laser pulses has indicated the competition of initiation, propagation, and termination within the 1-ms to 2-s time domain. Vesicle solutions have been found to be restored, therefore, to a new equilibrium of monomers, polymers, and photoproducts prior to the arrival of the next laser pulse at a 2-Hz repetition rate. Applying the energy in successive, essentially equal increments has allowed expressing the data in terms of

$$M(n) = M_0(1 - \eta)^n \quad (1)$$

where n, $M(n)$, and M_0 are the numbers of equienergy laser pulses, the remaining nonpolymerized surfactant after n pulses, and the initial surfactant, respectively. η, the fraction of the double-bonded monomers consumed after the photochemical events induced by a single laser pulse had subsided, is defined by

$$\eta = \Phi_r \epsilon E k_p/(k_m + k_s) \quad (2)$$

where Φ_r is the quantum efficiency of styryl radical formation, ϵ is the extinction coefficient at 266 nm, and E is the average energy/cm^2 of the laser pulse; k_p, k_m, and k_s are rate constants for polymerization, monomer re-formation, and formation of nonpolymerized photoproducts. The obtained good linearity of the laser photopolymerization plots has justified the assessments of the average polymer chain length in the vesicles (i.e., the degree

0024-9297/85/2218-2005$01.50/0

of polymerization, $k_p/(k_m + k_s)$) by

$$\frac{\eta}{\Phi_r \epsilon E} = \frac{k_p}{k_m + k_s} \quad (3)$$

Substitution of appropriate experimental values into eq 3 has led to a rather small value of 22 ± 10 for the average degree of photopolymerization of 1.[8]

Advantage has been taken in the present work of spin-label and phosphorescence anisotropy techniques to obtain information on the morphological consequences of vesicle surface photopolymerizations.

Experimental Section

Preparation, purification, and characterization of 1,[8] 5-doxylstearic acid (FA(12,3)),[9,10] and 5-doxylphosphatidylcholine (PC(12,3)[9,10] have been described. 5-Doxylstearic was purchased from Molecular Probes, Junction City, OR, and used without further purification.

Deionized water was doubly distilled in an all-glass apparatus. The final stage of distillation included a superheated oxygenated quartz column. For light scattering doubly distilled water was additionally filtered through a 0.2-μm Millistak filter system (Millipore Corp.).

Vesicle preparation and polymerization followed the established procedures.[8] Experiments performed at Gottingen, Potsdam, and Zurich had identical methodologies. Hydrodynamic diameters of vesicles and their polymerized counterparts were maintained to be 1200 ± 300 Å at each location (monitored by dynamic laser light scattering).

Compound 1 and the spin-label (300:1 mole ratio) were mixed in $CHCl_3$, and the solvent was removed by rotary evaporation. The lipid film was dried under vacuum and the dispersion was made by adding the appropriate amount of H_2O at ~60 °C to the dry lipid film and vortexing. Either the milky dispersion was used as such or it was sonicated for 1 h at ~50 °C by using a Branson B12 sonicator with a microtip. Undispersed material and titanium released from the microtip were removed by centrifugation at 12000*g* for 10 min. Alternatively, spin-labeled 1 dispersions were prepared by rotary evaporating a solution of the spin-label in organic solvent in a round-bottom flask and adding the ready-made 1 dispersion to the dry film of the spin-label (mole ratio of 1:label = 7:300). The spin-label was incorporated into the 1 dispersion at about 40 °C by gently rotating the round-bottom flask overnight. Both methods of incorporating the spin-label into 1 dispersions gave similar results. Polymerized 1 dispersions were spin-labeled by the latter method; i.e., the spin-label was incorporated into the ready-made polymerized dispersion. This was necessary because photopolymerization by irradiating the spin-labeled 1 dispersion with a xenon lamp (250 W, distance ≃ 30 cm) for 2–3 h destroyed the paramagnetic center. The degree of photopolymerization of 1 dispersions was monitored by measuring the absorbance of the vinyl double bond at 250 nm on a Unicam SP 1700 UV spectrophotometer.

Time-resolved rotational anisotropies of vesicle-incorporated erythrosin were performed in Gottingen and Potsdam. The Gottingen system, described in detail elsewhere,[11] monitors rotational diffusion via luminescence resulting from triplet-state decay. The Potsdam system utilized the Nd:YAG-based nanosecond flash photolysis system described elsewhere[8,12] for transient dichroism measurements. A polarizing beam splitter (Karl Lambrecht SBTAA 12-45 Glan-Thompson type) was placed in the analyzing beam path between the monochromator and detector. The beam splitter transmits vertically polarized light straight through and splits horizontally polarized light off on a 45° angle. Two RCA 1P28 (or Hammamatsu R928) photomultiplier tubes were used to monitor directly the intensities of parallel, I_z, and perpendicular, I_x, light transmitted. The output signal amplitudes of the photomultiplier-tubes were matched to each other for pure unpolarized light by translational adjustments of the polarizing beam splitter. Fine adjustments were made with the fine control adjustment of the rotational stage on which the beam splitter was mounted. The photomultiplier tube outputs were terminated in 50-Ω BNC throughput connectors. Once the network was balanced and the proper half-wave plate on the laser prism separator was set to ensure vertical laser polarization, data were collected in two steps. First, just the I_z signal was obtained. Normally, averaging the traces from 5–15 laser shots via program TEK[12] ensured sufficiently smooth data. Once the I_z signal was collected and stored on disk, the I_x signal was fed into the negative input on the oscilloscope's 7A13 differential comparator amplifier. This yielded the $I_z - I_x$ signal directly, which was averaged and stored. Program TRANIX has been developed to calculate and analyze the time-dependent rotational anisotropy function, $r(t)$.[12]

EPR measurements were carried out at 9.2 GHz with a Varian X-band spectrometer (Model E-104A) fitted with a variable-temperature control. The temperature was monitored with a thermocouple and was accurate to ±1 °C. EPR spectra were evaluated as described previously.[9] The calorimetric measurements were performed on a Perkin-Elmer differential scanning calorimeter (DSC-2 Perkin-Elmer, Kusnacht, Switzerland) as described before.[10]

Results and Discussion

Transient Dichroism of Erythrosin in Vesicles and Polymerized 1 Vesicles. Transient dichroism of erythrosin in vesicles and polymerized vesicles was determined by adding stock solutions of erythrosin to *already formed* vesicles or to already polymerized vesicles. Stoichiometric concentrations of erythrosin and 1 were kept at 1.67×10^{-7} and 1.96×10^{-3} M, respectively. This gave an estimated average of 12 erythrosin molecules per vesicle.

The time dependence of the polarization anisotropy, $r(t)$, is expressed by

$$r(t) = (GI_z - I_x)/(GI_z + 2I_x) \quad (4)$$

where I_z and I_x are the intensities of parallel and perpendicularly polarized light (luminescence intensities for measurements in Gottingen, transient triplet absorbances for measurements in Potsdam) and G is a correction factor for compensating against optical discrimination. A value for G was determined by measuring the anisotropy of erythrosin in water for both anisotropy apparatus. Since erythrosin in water rotationally reorients faster than 1.0 ns, it should give a constant value of zero for the anisotropy over the 0.5-ms full scale time used.

In unpolymerized 1 vesicles erythrosin showed no measurable anisotropy over the time scales employed (Figure 1). Conversely, erythrosin showed remarkable anisotropies if added to polymerized vesicles (Figures 2 and 3). At room temperature (Figure 2A) $r(t)$ rose to a plateau value over the 0.5-ms scale with a calculated exponential rise time of about 95 μs. At higher temperatures the plateau was lost and the anisotropy decay became measurable (Figure 2, parts C–H). Above 41 °C the decay of $r(t)$ was found to predominate and the buildup became too fast to measure. After the erythrosin-containing polymerized 1 vesicle solution was cooled to room temperature, the original anisotropy was not recovered; the anisotropy curve resembled those obtained at higher temperature. Reheating the solution and redetermining the anisotropies at different temperature yielded anisotropies shown in Figure 3.

Table I summarizes the anisotropy lifetimes for erythrosin in polymerized vesicles, for both the initial heating and reheating phases of the experiment. Anisotropy lifetimes shown in Table I were calculated by breaking the curves into the rising and falling portions and calculating the τ_R values separately. This is a good approach because the two apparent anisotropy lifetimes at each temperature are separated from each other by well over an order of magnitude, so that the long lifetime appears roughly constant over the scale of calculation for the short lifetime, whereas the latter is damped virtually down to zero over the scale of analysis for the long component.

The rising anisotropy curves in Figure 2 semed exceedingly peculiar at first glance and looked as if they con-

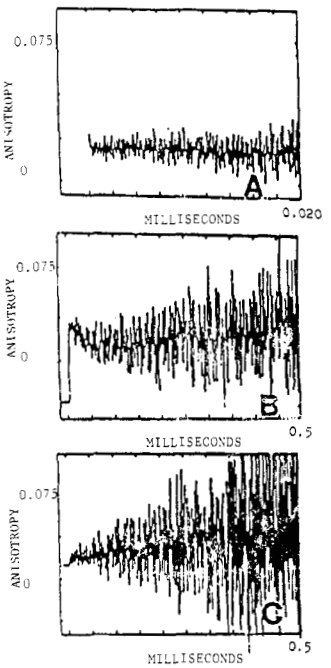

Figure 1. Anisotropy, $r(t)$, of erythrosin added to unpolymerized sonicated vesicles prepared from 1: (A) 25 °C, 0.020-ms full scale; (B) 25 °C, 0.5-ms full scale; (C) 42 °C, 0.5-ms full scale.

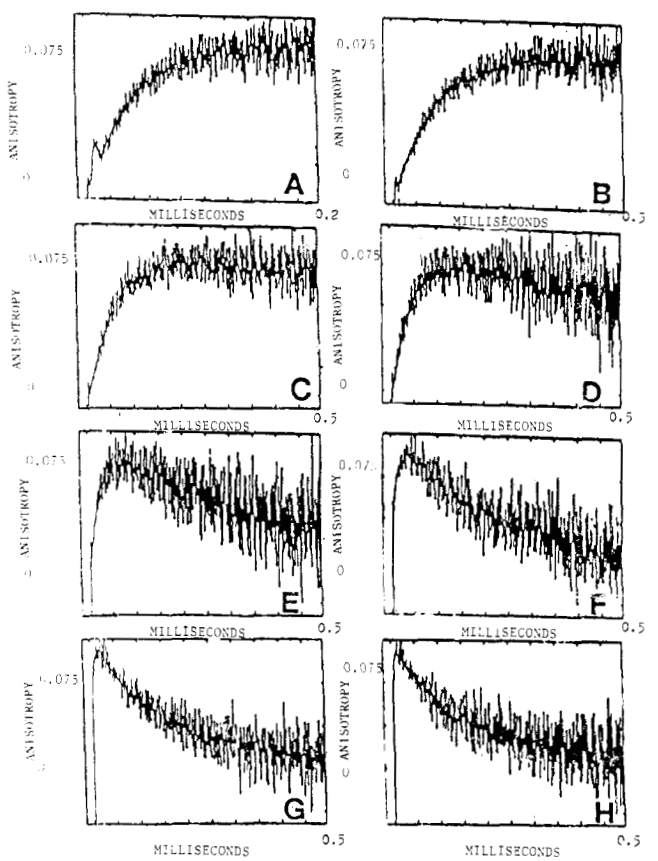

Figure 2. Anisotropy, $r(t)$, of erythrosin added to sonicated polymerized vesicles prepared from 1. First heating. Curve A is on 0.2-ms full scale; all other curves are on 0.5-ms full scale. (A) 25 °C; (B) 29 °C; (C) 33 °C; (D) 37 °C; (E) 41 °C; (F) 45 °C; (G) 50 °C; (H) 55 °C.

tradicted the whole notion of anisotropy as a quantity that decays by rotational orientation randomization. According to its definition, the anisotropy curve, $r(t)$, could only increase in time if the initially excited dipoles proceed to order themselves even more closely about the z axis! As

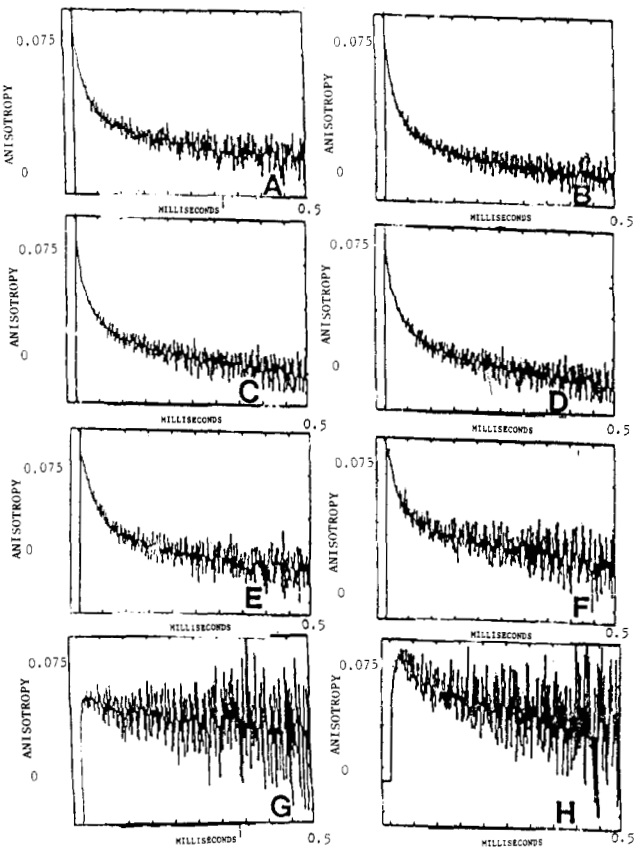

Figure 3. Anisotropy, $r(t)$, of erythrosin in the same polymerized vesicles of 1 as in Figure 2. The solution was cooled to room temperature and then reheated. All measurements were done on the 0.5-ms full scale. (A) 25 °C; (B) 30 °C; (C) 36 °C; (D) 42 °C; (E) 48 °C; (F) 54 °C; (G) 60 °C; (H) 66 °C.

Table I
Summary of Anisotropy Lifetimes for Erythrosin in Unpolymerized and Polymerized Surfactant Vesicles Prepared from 1[a]

system	temp, °C	τ_{R1}, μs	F_1[b]	τ_{R2}, μs
erythrosin in unpolymerized vesicles[c]	25			
	42			
erythrosin in polymerized vesicles, first heating	25	95	1.0	
	29	89.6	1.0	
	33	54.8		1200
	37	34.3		512
	41	17.2		482
	45	8.4		267
	50	3.0		169
	55	1.9		147
erythrosin in polymerized vesicles, reheat	24	11.3	0.66	185.7
	30	18.9	0.64	187.3
	36	23.7	0.61	228.6
	42			
	48	30.3	0.61	283.0
	54	25.8	0.57	568.7
	60	303.0	0.34	1137.0
	66	213.0	1.0	
	75	69	1.0	

[a] 1500-Å-diameter vesicles prepared from [1] = 1.96×10^{-3} M. Added [erythrosin] = 1.6×10^{-7} M. [b] Fraction of τ_{R1}. [c] No observed anisotropy.

there are no externally applied fields to define a preferred orientation in space, such arbitrary spatial organization should clearly be impossible. The data could be rationalized, however, quite readily by assuming the partitioning of erythrosin among different environments with differing fluorescence lifetimes and anisotropies.

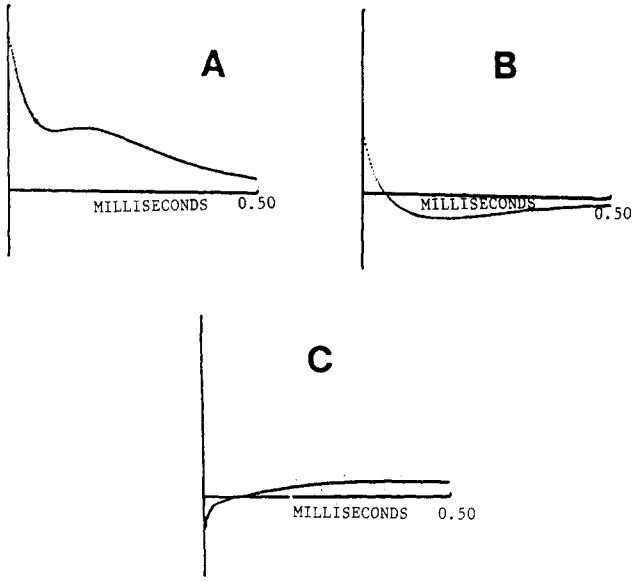

Figure 4. Computer-generated anisotropy curves according to eq 8. Some curves of $r(t)$ for systems with a fluorscent species partitioned among three different environments. These were calculated by program MULTEX according to eq 4: (A) $\tau_1 = 38$ μs, $\tau_{R1} = 1.0$ μs, LAM (angle between absorption and emission dipoles in degrees) = 0.10; $\tau_2 = 40.0$ μs, $\tau_{R2} = 40$ μs, LAM = 0.80; $\tau_3 = 200$ μs, $\tau_{R2} = 200$ μs, LAM = 0.10. (B) $\tau_1 = 400$ μs, $\tau_{R2} = 200$ μs, LAM = 0.40; $\tau_2 = 100$ μs, $\tau_{R2} = 75$ μs, LAM = 0.40; $\tau_3 = 30$ μs, $\tau_{R2} = 30$ μs, LAM = 0.20. (C) $\tau_1 = 200$ μs, $\tau_{R1} = 500$ μs, LAM = 0.20; $\tau_2 = 200$ μs, $\tau_{R2} = 200$ μs, LAM = 0.50; $\tau_3 = 50$ μs, $\tau_{R3} = 10$ μs, LAM = 0.30.

If there are N different fluorescing species (which can also mean one single fluorescent molecule in N different microenvironments), each having its own emission decay time τ_i (fluorescence or phosphorescence), its own anisotropy decay function $C_{2,0,i}(t)$, and its own angle between emission and absorption dipoles λ_i, then the time-dependent decays of the parallel and perpendicularly polarized light intensities are given by

$$I_z(t) = \sum_{i=1}^{N} \tfrac{1}{3} + \tfrac{4}{15} C_{2,0,i}(t) e^{-t/\tau_i} \quad (5)$$

$$I_x(t) = \sum_{i=1}^{N} \tfrac{1}{3} + \tfrac{2}{15} C_{2,0,i}(t) e^{-t/\tau_i} \quad (6)$$

and hence $r(t)$ is expressed as

$$r(t) = \frac{\tfrac{2}{5} \sum_{i=1}^{N} e^{-t/\tau_i} C_{2,0,i}(t)[(3 \cos^2 \lambda_i - 1)/2]}{\sum_{i=1}^{N} e^{-t/\tau_i}} \quad (7)$$

If, as is a good approximation for a molecule like erythrosin, each anisotropy function $C_{2,0,i}(t)$ can be represented by a single exponential with a characteristic rotational reorientation time of $\tau_{R,i}$, then eq 7 becomes

$$r(t) = \frac{\tfrac{2}{15} \sum_{i=1}^{N} e^{-t/\tau_i} e^{-t/\tau_{R,i}}[(3 \cos^2 \lambda_i - 1)/2]}{\sum_{i=1}^{N} e^{-t/\tau_i}} \quad (8)$$

Program MULTEX was written to plot $r(t)$ for any given set of parameters τ_i, $\tau_{R,i}$, λ_i, and N.[13] The number of different forms that $r(t)$ can take when many components are involved is remarkable. Figure 4 illustrates some of these diverse forms for different combinations of the parameters in eq 4. Table II gives the luminescence lifetimes of the erythrosin probes for a few selected temperatures. The

Table II
Luminescence Lifetime Values for the Erythrosin Probe in Different Media

$$(I_z + 2I_x) = F_1 e^{-t/\tau_1} + F_2 e^{-t/\tau_2} + F_3 e^{-t/\tau_3}$$

system	temp, °C	τ_1, ±s	F_1	τ_2, ±s	F_2	τ_3, ±s	F_3
erythrosin in water	25	84.0	1.0				
erythrosin in polymerized vesicles	25	10.0	0.30	172.0	0.23	39.3	0.47
	41	8.3	0.56	199.0	0.22	31.9	0.22
	50	6.8	0.55	182.0	0.24	36.3	0.21
	55	5.7	0.65	124.0	0.13	28.1	0.22
erythrosin in unpolymerized vesicles, first heating	25	8.3	0.12	113.0	0.64	43.7	0.24

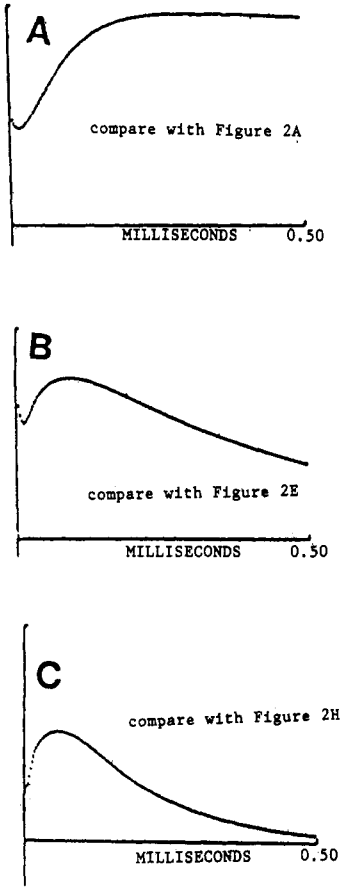

Figure 5. Computer-generated anisotropy curves using data given in Tables I and II. (A) $\tau_1 = 10$ μs, $\tau_{R1} = 95$ μs, LAM = 0.30; $\tau_2 = 172$ μs, $\tau_{R2} = 10000$ μs, LAM = 0.23; $\tau_3 = 39.3$ μs, $\tau_{R3} = 1.0$ μs, LAM = 0.47. (B) $\tau_1 = 8.3$ μs, $\tau_{R1} = 17.2$ μs, LAM = 0.50; $\tau_2 = 100$ μs, $\tau_{R2} = 482$ μs, LAM = 0.22; $\tau_3 = 31.9$ μs, $\tau_{R3} = 1.0$ μs, LAM = 0.22. (C) $\tau_1 = 5.7$ μs, $\tau_{R1} = 1.0$ μs, LAM = 0.65; $\tau_2 = 124$ μs, $\tau_{R2} = 147$ μs, LAM = 0.13; $\tau_3 = 28.1$ μs, $\tau_{R3} = 1.0$ μs, LAM = 0.22.

I_z and I_x curves were combined according to $I_z + 2I_x$ to eliminate anisotropy effects, and the resulting curves were analyzed into three exponentials. Combination of the data given in Tables I and II led to the computer-generated curves shown in Figure 5. The curves shown in Figure 5 closely match the form of the experimental curves in Figure 2 for the assignments of the $\tau_{R,i}$ to the τ_i indicated in the computer-generated curves. It was not necessary to assume a nonalignment between absorption and emission dipoles to match the forms of the experimental and computer-generated curves.

The anisotropy curves of erythrosin in polymerized vesicles at different temperatures are now rationalized in the following way: The short component, τ_1 in Table II,

probably corresponds to erythrosin residing very near to the vesicle surface and associated with the polymer chains. The luminescence lifetime may be short compared to the other two due to an energy transfer from the erythrosin triplet to the ring system of the styrene polymers. Its corresponding anisotropy lifetime, τ_{R1} in Table I, would indicate that the probe's rotation is hindered by its proximity to the polymer.

The lifetime τ_3 in Table II is taken to correspond to erythrosin in an aqueous environment, probably in the charge layer around the vesicle. The value of τ_3 (ca. 40 μs) is the closest of the three luminescence lifetimes to the one-component lifetime of erythrosin in pure water (about 80 μs). The probability that τ_3 represents erythrosin in a watery environment is supported by the fact that a small anisotropy lifetime (ca. 1 ns) must be entered in MULTEX for the 40-μs component in order to match the experimental curves in Figure 2. The anisotropy lifetime of erythrosin has been measured in the course of this work via fluorescence depolarization and is about 1 ns.

The phosphorescence lifetime τ_2 in Table II is more than double that in pure water. It is a general trend among xanthene dyes and many other ionic fluorescent molecules that their excited singlet and triplet states become somewhat stabilized, i.e., live longer, in apolar solvents[13] (e.g., τ_F for rose bengal: 143 ± 40 ps (H_2O), 1440 ± 100 ps (MeOH), 7100 ± 200 ps (propylene glycol)). In polar environments the excited states are destabilized probably because of the ionic and dipolar electric field perturbations on the state. Such perturbing fields are much smaller in apolar solvents. It is thus very plausible that the long luminescence component, τ_2, is due to erythrosin lodged among the hydrocarbon chains of the polymerized vesicle. Further evidence of this is given by the fact that the long anisotropy lifetime, τ_{R2} in Table I, must be matched with the long luminescence lifetime τ_2 in order to match the experimental anisotropy curves for the polymerized vesicles. Up to 33 °C the long anisotropy component τ_{R2} is not even measurable on the 0.5-ms scale; i.e., it must be at least several milliseconds long. In fact the existence of an anisotropy lifetime longer than the full scale of observation is the only means by which $r(t)$ can reach a nonzero plateau that stays flat up to the end of the observation. Ultimately $r(t)$ must go to zero at long enough times if the luminescing system does not have a frozen orientation in space. In this case, the ultimate reorientation of the erythrosin in the bilayer must be linked to the full rotation of the vesicle. Since temperatures below about 33 °C are below the phase transition temperature for these vesicles, the erythrosin molecules lodged in the hydrocarbon layer are actually in a fairly well-ordered gel-type environment in which there is little or no fluidity to allow them to rotationally reorient. The erythrosin is thus locked to the vesicle and its rotational reorientation below the phase transition temperature.

The phase transition temperature of these polymerized vesicles can be roughly determined, in fact, by plotting the anisotropy lifetimes, τ_{R1} and τ_{R2}, vs. temperature. As seen in Figure 6, there is a sharp drop in anisotropy lifetimes over the range of about 33–37 °C. In the proposed interpretation the speeding up of the anisotropy lifetimes indicates that the hydrocarbon bilayer in which the erythrosin is lodged has become fluidlike and allows a hindered rotation of the probe which is nonetheless still faster than the complete vesicle rotational reorientation time. Using

$$\frac{1}{\tau_R} = \frac{k_B T}{V\eta} = 6D \qquad (9)$$

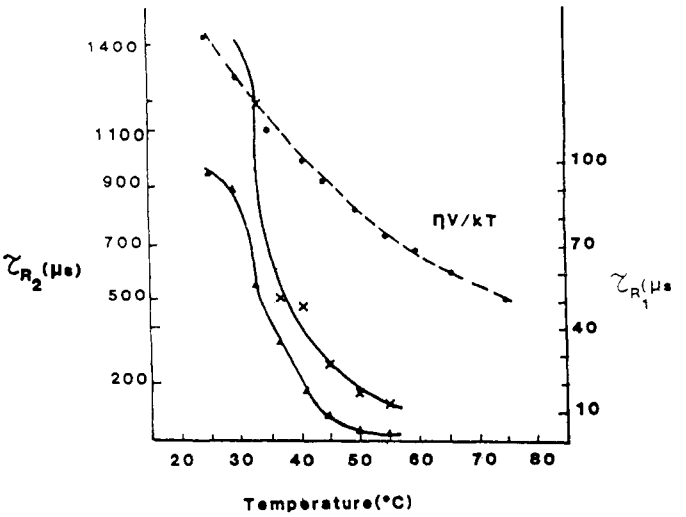

Figure 6. τ_{R1} and τ_{R2} of erythrosin in polymerized vesicles of 1 vs. temperature. Note the phase transition between 30 and 40 °C of the hydrocarbon chains. The dashed line shows the expected behavior of τ_{R1} and τ_{R2} vs. temperature if τ_R were due merely to the vesicle's rotational reorientation (eq 9). (▲) τ_{R1}; (×) τ_{R2}.

where k_B is Boltzmann's constant, T is the absolute temperature, V is the molecular volume, and η is the viscosity, leads to a τ_R value on the order of a millisecond for 1600-Å-diameter vesicles. This would explain the nondecay of the plateau for the $r(t)$ curves of polymerized vesicles below about 33 °C. That the behavior of the curve of τ_R vs. temperature in Figure 6 corresponds to a true phase transition, and not just to increased vesicle rotational reorientation, is made clear by plotting on the dashed curve the value of τ_R vs. temperature as calculated by eq 9. The dashed curve was normalized to cross the experimental curve at 33 °C.

What yet needs to be explained is why the erythrosin with unpolymerized vesicles does not show any anisotropy behavior at all on the time scales of observation. For erythrosin in unpolymerized vesicles the first two phosphorescence lifetimes, τ_1 and τ_3 in Table II, are very similar to τ_1 and τ_3 for the case of polymerized vesicles. In analogy, then, τ_1 and τ_3 correspond to erythrosin present in the vesicle charge layer and associated with the head group, respectively. Absence of anisotropy of the surfactant head group associated erythrosin is due to the fact that the monomeric head groups are very "floppy" in the unpolymerized vesicles (they reorient on the nanosecond time scale). The rotational reorientation of the probe in polymerized vesicles, in contrast, was highly impeded by its association with rather rigid polymer chains about the head groups.

The third phosphorescence lifetime, τ_3, for the erythrosin in unpolymerized vesicles is fairly close to the value obtained for the probe in pure water. As there is no corresponding long anisotropy lifetime, as there was in the polymerized case, the case for assigning τ_3 to the presence of erythrosin in the purely aqueous phase (i.e., away from vesicles) or far out in the vesicle charge layer is strengthened. What seems certain in the unpolymerized vesicle case is that, judging by the lack of any anisotropy on the time scale of observation, the erythrosin probe does not enter into the type of tight association with the unpolymerized vesicles that it does with polymerized vesicles. As mentioned τ_{R1} for the unpolymerized vesicles is very fast because there are no surface polymer chains to hinder the probe. The fact that neither τ_2 nor τ_{R2} in polymerized vesicles corresponds to its counterpart in nonpolymerized vesicles indicates that the probe does not penetrate into

the hydrocarbon interior of the unpolymerized vesicles. This follows from the argument made earlier identifying the long τ_2 and τ_{R2} with erythrosin lodged in the hydrocarbon bilayers of polymerized vesicles.

The static and dynamic light scattering data on vesicles prepared from 1 showed that the inter-head group spacing in the unpolymerized vesicles is about 10 Å.[8] Polymer chemists have extensively studied the physical properties of styrene polymers and determined the interstyrene separation to be about 4.2 Å.[15] Taking into acount the styrene to methyl and methyl to nitrogen bonds in monomer 1 the inter-head group spacing in polymerized vesicles should be about 7.5 Å. Thus, the polymerization process draws bonded head groups closer to one another and inevitably causes corresponding greater separations between other monomers. *The net result of polymerization on vesicle surface morphology is to create a state of surface inhomogeneity in which bonded monomers are closer together than in the unpolymerized state and shallow clefts are formed in the surface that expose the hydrocarbon bilayer chains to water and solutes.* This now explains why a fraction of the erythrosin probe is in the hydrocarbon layer: The clefts that have opened up due to the vesicle polymerization admit the solubilized erythrosin, thus entrapping and immobilizing it and also stabilizing its triplet state somewhat due to the reduced polarity of the environment. Close packing of the surfactant chains in the unpolymerized vesicles may prevent the entry of erythrosin below the phase transition temperature of the vesicles.

The observed hysteresis (compare Figures 2 and 3) may imply vesicle "annealing". Since the proposed surface clefts are probably shallow, in the sense that only the first half dozen or so carbons on the chains assume the gauche kinks necessary to open and maintain the clefts, after the phase transition the kinks and chain disorder are distributed throughout the chains with the net effect that the clefts become much deeper, narrower, and statistically more uniform in size. Water may also penetrate more deeply into the vesicle bilayer, and upon cooling, these new characteristics of the clefts may well be largely maintained. The vesicle has been "annealed". The erythrosin probe then becomes wholly associated with the vesicle, the water now allowing penetration further into the bilayer. The two probe environments become deep seating in the bilayer and associating around the head group portion of the clefts. The curves of $r(t)$ in Figure 3A–F are seen to vary only slightly as the temperature is raised. Both the short and long rotational lifetimes, τ_{R1} and τ_{R2}, become somewhat longer, but no drastic changes are seen as, for example, upon the first heating when passing through the phase transition temperature (Figure 2A–F). The slight lengthening of the lifetimes in Figure 3A–F may indicate that the erythrosin accommodates itself and immobilizes itself better in the clefts when the temperature and movement of the chains increase. The fact that the clefts still do exist after "annealing" is supported by the fact that there is still a measurable well-defined anisotropy, whereas for unpolymerized vesicles there is no anisotropy signal on the available time scales of meausurement.

Electron Paramagnetic Resonance Spectroscopic Investigations of Spin-Labels in 1 Vesicles. Effect of Polymerization. EPR spectra of sonicated vesicles prepared from 1 and labeled with FA(12,3) or PC(12,3) are shown in Figure 7. The spectra at 42 °C are typical for the spin-label being present in a liquid crystalline lipid bilayer and undergoing fast but anisotropic motion. In contrast, at room temperature immobilized EPR spectra

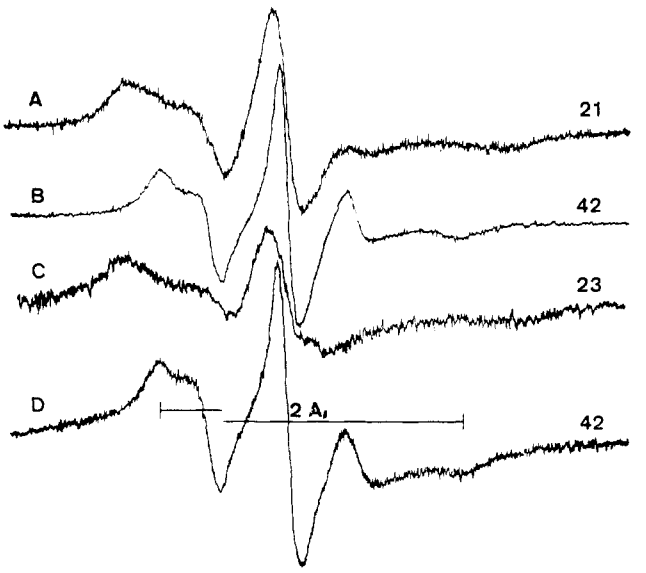

Figure 7. ESR spectra of sonicated 1 dispersions in H_2O labeled either with FA(12,3) (spectra A and B) or with PC(12,3) (spectra C and D). The concentration of the 1 dispersion was 10 mg/mL (mole ratio of label:1 = 1:300). Temperatures (°C) are given on the right.

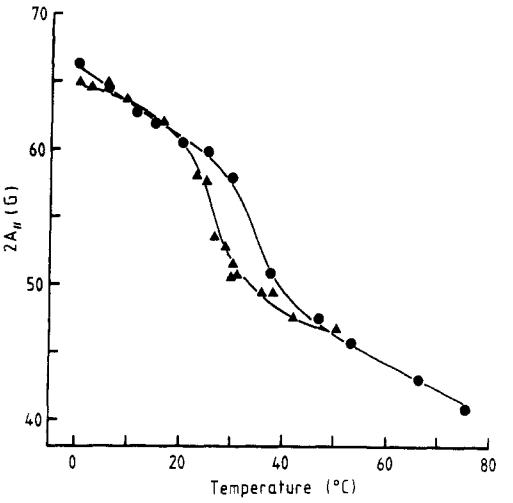

Figure 8. Temperature dependence of the maximum hyperfine splitting $2A_{II}$ of FA(12,3)-labeled, sonicated dispersions of 1 in H_2O. A_{II} was taken directly from the EPR spectrum as shown in Figure 7. The concentration of 1 was 10 mg/mL; (▲) unpolymerized; (●) polymerized.

were obtained (Figure 7A,C). With both spin probes used the value of the hyperfine splitting constant A_{II} was 32–34 G, approaching the A_{zz} tensor component. This indicates that under these conditions the rapid rotation of the spin probe about its molecular long axis or bilayer normal is frozen. The temperature dependence of the maximum hyperfine splitting $2A_{II}$ of FA(12,3)- and PC(12,3)-labeled 1 vesicles is shown in Figures 8 and 9, respectively. Both labels indicate that 1 undergoes a phase transition, the temperature of which is 26.5 and 31.0 °C for the FA(12,3)- and PC(12,3)-labeled 1 vesicles, respectively. Below the transition temperature (T_C) the maximum hyperfine splittings $2A_{II}$ increased rapidly to values ≥60 G. Right above the T_C point $2A_{II}$ values of about 50 G were measured (Figures 8 and 9), which are characteristic of liquid-crystalline lipid bilayers. Both the line shape of the EPR spectra and the values of the maximum hyperfine splitting $2A_{II}$ below and above the T_C point are consistent with the transition being a gel-to-liquid crystal transition.[10]

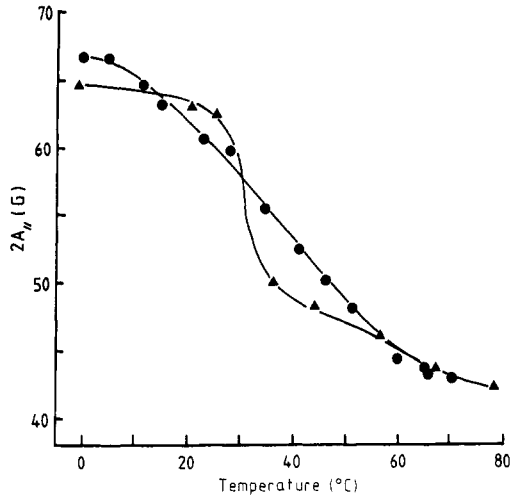

Figure 9. Temperature dependence of the maximum hyperfine splitting $2A_{II}$ of PC(12,3)-labeled, sonicated dispersions of 1 in H_2O (concentration was 10 mg/mL): (▲) unpolymerized; (●) polymerized.

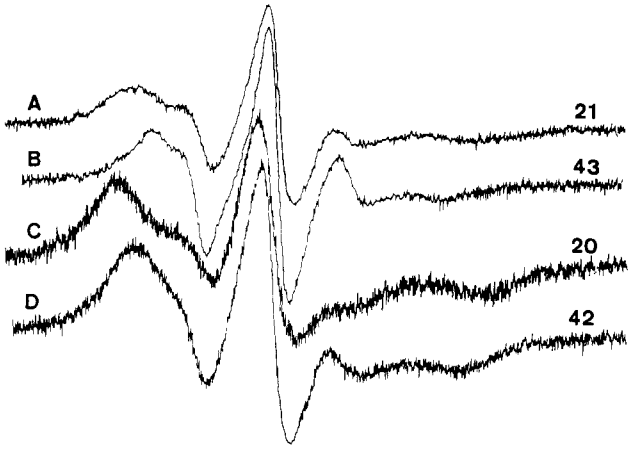

Figure 10. ESR spectra of sonicated and polymerized 1 dispersions in H_2O labeled either with FA(12,3) (spectra A and B) or with PC(12,3) (spectra C and D). The concentration of the 1 dispersion was 10 mg/mL (mole ratio of label:1 ≃ 1:300). Temperatures (°C) are given in the right.

EPR spectra of polymerized 1 vesicles labeled with either FA(12,3) or PC(12,3) are shown in Figure 10. The spectra of the FA(12,3)-labeled polymerized vesicles are almost superimposable with the corresponding spectra from unpolymerized samples (Figures 7 and 10). This result suggests that the polymerized domains are freely accessible to the fatty acid spin probe. A comparison of the polymerized and nonpolymerized samples (Figures 7 and 10) shows a qualitative difference at room temperature; the spectra from the polymerized sample appear to be less immobilized than those from the unpolymerized one. This phenomenon, which was observed reproducibly, is at first difficult to rationalize. It is, however, consistent with the interpretation of the cleft formation discussed in detail above. The EPR spectra of the PC(12,3)-labeled polymerized 1 vesicles at temperatures >40 °C show some dipolar line broadening. This could be due to a reduction in accessibility of the spin probe to the polymerized domains.

The effect of polymerization upon the temperature dependence of the maximum hyperfine splitting $2A_{II}$ is shown in Figures 8 and 9. For the FA(12,3)-probed 1 dispersions, the transition was shifted to higher temperatures, from 26.5 to 35 °C. Polymerization had little, if any, effect on the $2A_{II}$ values above and below the transition region (Figure 8). For PC(12,3)-probed vesicles the effect of polymerization was more dramatic (Figure 9). After polymerization the $2A_{II}$ values decreased almost linearly with increasing temperatures. The transition region appears to be spread out over a much greater temperature range. Only at temperatures >60 °C were the $2S_{II}$ values consistent with those measured with unpolymerized 1 vesicles. By the same criterion, the motional anisotropy appears increased in the temperature range of about 30–60 °C (Figure 9).

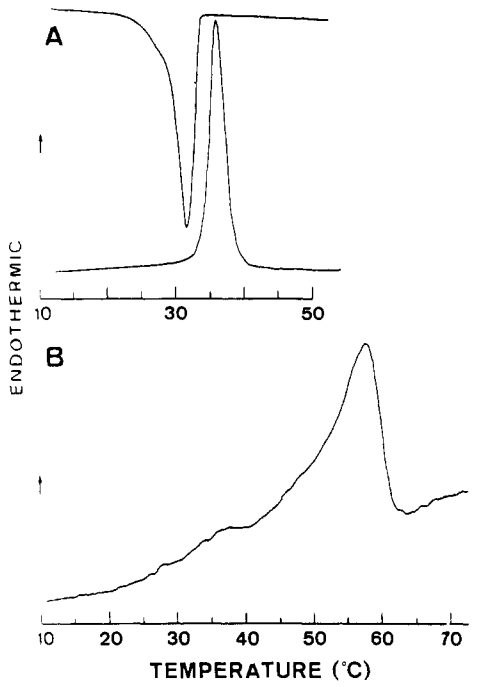

Figure 11. (A) Differential scanning calorimetry heating and cooling curves of an unsonicated dispersion of 1 in H_2O (54.3 mg/mL). Heating/cooling rate = 5 °C/min. (B) Same sample as in (A) after dilution and photopolymerization (20 mg/mL).

Differential Scanning Calorimetry. Differential scanning calorimetry could only be carried out on somewhat higher concentrations of multicompartment 1 vesicles, prepared by vortexing 1 with water (i.e., no sonication). Reproducible sharp, endothermic order–disorder transitions at 35 ± 1 °C[16] with an enthalpy change ΔH = 11.5 + 1 kcal/mol were observed for unpolymerized vesicles (Figure 11A). In the light of the EPR results discussed above this transition can be assigned to a gel-to-liquid crystal transition. When the sample was cooled, a sharp exothermic transition was observed, with the transition temperature depressed by 3–4 °C compared to the transition temperature on heating and with a shoulder at the end of the exothermic transition (Figure 11A). Both the endothermic and exothermic transition were reproducible on successive heating and cooling cycles, respectively. The effect of photopolymerization on the thermal behavior of unsonicated 1 dispersions is illustrated in Figure 11B. Polymerized 1 dispersions gave reproducibly broad endotherms spread out over the temperature range of about 30–63 °C with a peak temperature of about 59 °C. Similar broad exothermic transitions were observed upon cooling, with the peak temperature being depressed by about 7 °C (data not shown). The effect of polymerizing 1 in the polar group is to increase the gel-to-liquid crystal transition temperature by about 25 °C. This behavior may well imply the intrabilayer polymerization in the multicompartment vesicles.

Acknowledgment. We acknowledge the expert technical assistance of Y. Baumann. Support of this work by

the National Science Foundation and by the Schweizer Nationalfond is gratefully acknowledged. The generous support of Tom Jovin and his excellent triplet facility in Gottingen is likewise acknowledged.

Registry No. 1, 88703-85-9; FA(12,3), 29545-48-0; PC(12,3), 66642-40-8; erythrosin, 16423-68-0.

References and Notes

(1) Clarkson University. Present address of W.R.: Department of Physics, Tulane University, New Orleans, LA 70118. Present address of J.H.F.: Department of Chemistry, Syracuse University, Syracuse, NY 13210.
(2) Eidgenossische Technische Hochschule.
(3) Fendler, J. H.; Tundo, P. *Acc. Chem. Res.* **1984**, *17*, 3-7.
(4) Fendler, J. H. In "Surfactants in Solution"; Mittal, K. L., Lindman, B., Eds.; Plenum Press: New York, 1984.
(5) Gros, L.; Ringsdorf, H.; Schupp, H. *Angew. Chem., Int. Ed. Engl.* **1981**, *20*, 305-325.
(6) Fendler, J. H. *Science (Washington, D.C.)* **1984**, *223*, 888-894.
(7) Fuhrhop, J. H.; Mathieu, J. *Angew. Chem., Int. Ed. Engl.* **1984**, *23*, 100-113.
(8) Reed, W.; Guterman, L.; Tundo, P.; Fendler, J. H. *J. Am. Chem. Soc.* **1984**, *106*, 1897-1907.
(9) Hauser, H.; Gains, N.; Semerra, G.; Spress, M. *Biochemistry* **1982**, *21*, 5621-5628.
(10) Hauser, H.; Palfrauf, F.; Shipley, G. G. *Biochemistry* **1982**, *21*, 1061-1067.
(11) Austin, R. H.; Karohl, J.; Jovin, T. M. *Biochemistry* **1983**, *22*, 3082-3090.
(12) Reed, W. Dissertation, Clarkson University, Potsdam, NY, 1984.
(13) Robbins, R. J.; Fleming, G. K.; Beddard, G. S.; Robinson, G. W.; Thistlethwaite, P. J. *J. Am. Chem. Soc.* **1980**, *102*, 6271-6279. VonJena, A.; Lessing, H. E. *Chem. Phys. Lett.* **1981**, *78*, 187-193.
(14) Reed, W.; Politi, M. J.; Fendler, J. H. *J. Am. Chem. Soc.* **1981**, *103*, 4591-4593.
(15) David, C.; Baeyans-Volant, D. *Ann. N.Y. Acad. Sci.* **1981**, *366*, 341-355.
(16) Peak temperatures in the excess heat capacity curves were taken as the transition temperature.

Studies of the Antenna Effect in Polymer Molecules. 9. Energy Transfer, Migration, and Photoreactivity of Copolymers of 1-Naphthylmethyl Methacrylate and [2-(9,10-Anthraquinonyl)]methyl Methacrylate

Xiao-Xiu Ren† and James E. Guillet*

Department of Chemistry, University of Toronto, Toronto, Canada M5S 1A1.
Received December 10, 1984

ABSTRACT: Energy migration and transfer were investigated in 1-naphthylmethyl methacrylate polymers containing anthraquinone chromophores. The naphthalene singlet state is quenched by singlet energy migration and transfer to anthraquinone. Energy-transfer efficiencies of ca. 80% were obtained at acceptor mole fractions of 2%. These molecular antenna successfully mimic the energy-harvesting function of the antenna pigments of natural photosynthetic systems. The effect of copolymer composition on the efficiency of energy transfer, the quenching mechanism of the singlet, and the mechanism of the delayed fluorescence were studied. After their formation the anthraquinone triplet states are in turn quenched by triplet energy transfer to naphthalene, a process that leads to enhanced naphthalene phosphorescence intensity. The occurrence of cyclic energy transfer shows that both singlet and triplet migration and transfer occur in the same polymer chain. In THF solution at 25 °C the anthraquinone traps undergo rapid photoreduction to the corresponding hydroquinone.

The analogy between "antenna polymers", which consist of sequences of aromatic donor chromophores such as naphthalene or phenanthrene, and the "antenna pigments" in natural photosynthesis has been discussed in previous papers in this series.[1-10] In the latter system it is postulated that a regular arrangement of the chlorophyll molecules in the plant thylakoid membrane promotes rapid singlet energy migration to the active center where the excitation energy is used to drive a sequence of reactions leading to charge separation and the ultimate formation of high-energy products that are used as fuels by both plants and animals.[11] In previous work it has been shown that singlet energy migration can also take place within a single macromolecule in solution at high dilution and that the excitation can be trapped with efficiencies exceeding 80%, which is comparable to that estimated for the antenna pigments in plant chloroplasts. It has also been shown that the process takes place rapidly—on the order of 5–20 ns, a time scale that precludes any large movement of either the polymer chain or its side groups—and appears to be nearly as efficient in a solid organic glass at 77 K as in fluid solution at ambient temperature. Although triplet energy migration also occurs in aromatic polymers[12-14] by a mechanism now generally accepted, in this work the term "antenna effect" is restricted, by analogy with the natural photosynthetic system, to the migration and trapping of singlet excitons.[15]

In previous studies, anthracene was used as a trap, because its fluorescence emission could be used as a probe of the photophysics of the processes involved. Three studies in which phenyl ketone traps were used did not show enhanced reactivity of the ketone because of the rapid occurrence of "cyclic energy transfer" in which the singlet excitation transferred to the trap, after rapid intersystem crossing to the triplet, was efficiently quenched by the adjacent naphthalene groups.[7,10,16]

In the present work anthraquinone traps were used in a typical antenna polymer, poly(1-naphthylmethyl methacrylate) (P1NMMA). The traps were introduced by copolymerization with [2-(9,10-anthraquinonyl)]methyl methacrylate (2AQMMA). Copolymers of 2AQMMA with 2-naphthylmethyl methacrylate (2NMMA) had been prepared earlier by Nakahira et al.,[17] who showed that

† Current address: Polymer Department, Peking Institute of Chemical Technology, Peking, People's Republic of China.

0024-9297/85/2218-2012$01.50/0